

Role of Human Herpesvirus 8 Interleukin-6-Activated gp130 Signal Transducer in Primary Effusion Lymphoma Cell Growth and Viability

Emily Cousins, John Nicholas

Sidney Kimmel Comprehensive Cancer Center at Johns Hopkins, Department of Oncology, Johns Hopkins University School of Medicine, Baltimore, Maryland, USA

Human herpesvirus 8 (HHV-8) infection is associated with Kaposi's sarcoma, primary effusion lymphoma (PEL), and multicentric Castleman's disease. HHV-8-encoded viral interleukin-6 (vIL-6) is believed to contribute to pathogenesis via proproliferative, antiapoptotic, and proangiogenic activities. In PEL cells, vIL-6 is produced in functional amounts during viral latency and promotes the growth of these cells, mediating its activity from the endoplasmic reticulum (ER), where it is predominantly localized. This vIL-6 activity is dependent, in part, on its interaction with a splice variant of vitamin K epoxide reductase complex subunit 1 (VKORC1), termed VKORC1 variant 2 (VKORC1v2). Here we report that the IL-6 signal transducer, gp130, which can support vIL-6 signaling from the ER, is also required for optimal PEL cell growth and viability. Levels of activated extracellular regulated kinases (ERKs) 1 and 2 and signal transducer and activator of transcription 1 (STAT1) and STAT3, phosphorylated following gp130 stimulation, were reduced in gp130-depleted BCBL-1 and BC-1 cells. Diminished STAT activation was also detected in JSC-1 and BC-3 cells. Effects of gp130 depletion on growth could be mimicked by short hairpin RNA targeting of ERKs 1 and 2 or by depletion of STAT3. Finally, inhibition of vIL-6–gp130 association specifically within the ER compartment suppressed cell proliferation and viability, mirroring the effects of gp130 depletion. Combined, these data demonstrate that gp130, in addition to VKORC1v2, is essential for normal PEL cell growth and survival and that ER-localized vIL-6–gp130 interactions are critical for these activities. Targeting of intracellular vIL-6–gp130 interactions could potentially provide a means of PEL therapy.

Human herpesvirus 8 (HHV-8) encodes several proteins that are believed to contribute to the onset and/or progression of endothelial Kaposi's sarcoma (KS) and the B cell malignancies primary effusion lymphoma (PEL) and multicentric Castleman's disease (MCD) (1–4). Viral interleukin-6 (vIL-6), like its cellular counterparts, is a growth factor for B cells and other cell types and promotes inflammatory and angiogenic responses. These activities implicate the viral cytokine as a contributory factor in HHV-8-associated neoplasias (5, 6). In PEL cells, true latent expression of vIL-6 suggests that the viral protein can contribute to this disease in a direct, autocrine fashion by promoting PEL cell proliferation and survival, in addition to possibly maintaining latent viral reservoirs during normal (disease-free) infection (7, 8).

While the three-dimensional structures of vIL-6 and human IL-6 (hIL-6) are similar and both can bind to and induce dimerization of the gp130 signal transducer, vIL-6 is unique in that it is “preconformed” to mediate gp130 dimerization without first binding the nonsignaling gp80 IL-6 receptor subunit (9–11). However, vIL-6 can bind gp80 and form hexameric complexes (vIL-6₂–gp130₂–gp80₂) in addition to tetrameric (gp80-devoid) complexes (10, 12). Hexameric and tetrameric complexes have distinguishable signaling properties (13), likely mediated in part by gp80 stabilization of vIL-6-induced gp130 dimerization (10, 12). Within the endoplasmic reticulum (ER), vIL-6 induces the formation of tetrameric complexes exclusively (8, 14). ER-directed hIL-6 is unable to induce gp130 complexing and signal transduction. vIL-6, hIL-6, and other cellular IL-6 proteins activate STAT1 and STAT3 via gp130-associated Janus kinase (JAK)-mediated tyrosine phosphorylation of the transcription factors (15). Mitogen-activated protein kinase (MAPK) signaling is activated following SHP2 recruitment to gp130 and phosphorylation by JAK, which leads to downstream phosphorylation and activation of ERKs 1 and 2 (15). In addition to differences in the gp80

dependency of ligand-induced gp130 dimerization and the ability of vIL-6 to signal from the ER, inefficient secretion of vIL-6 distinguishes it from its cellular counterparts (14). Thus, vIL-6 is found largely intracellularly, specifically within the ER, and its ability to signal from this compartment suggests that this may be functionally important for both virus biology and viral pathogenesis. Indeed, vIL-6 depletion-mediated inhibition of PEL cell growth in culture can be reversed by transduction of ER-retained (KDEL motif-tagged) vIL-6 (8). Also, vIL-6 support of PEL cell growth can be inhibited by an ER-localized single-chain antibody specific to vIL-6 (16). It is reasonable to hypothesize that vIL-6 may contribute to PEL pathogenesis via gp130 signaling. STAT3, a major target of such signaling and a transcription factor implicated in many human cancers (17–19), is activated in PEL cells and appears to be important for their viability, in part via the STAT3-induced prosurvival protein survivin (20).

However, demonstration of vIL-6-mediated signal transduction via gp130 in PEL cells and the role of gp130 in PEL cell biology have not been reported. Recently, vIL-6 was found to interact with the ER membrane protein vitamin K epoxide reductase complex subunit 1 variant 2 (VKORC1v2), a splice variant of the warfarin target VKORC1 (variant 1) (21), and this interaction was shown to be important for the progrowth and antiapoptotic activities of vIL-6 in PEL cells (22). Interaction of vIL-6 with VKORC1v2 occurs via a transmembrane-proximal region of the ER luminal do-

Received 11 March 2013 Accepted 24 July 2013

Published ahead of print 31 July 2013

Address correspondence to John Nicholas, nichojo@jhmi.edu.

Copyright © 2013, American Society for Microbiology. All Rights Reserved.

doi:10.1128/JVI.02047-13

main; its precise mapping enabled the development of a vIL-6-refractory variant and an interaction-inhibitory peptide that helped reveal the functional relevance of the vIL-6–VKORC1v2 interaction (22). The mechanism of vIL-6 activity via VKORC1v2 appears to be independent of gp130.

In the present study, we have investigated directly the influence of gp130 on PEL cell proliferation and viability, the role of vIL-6–gp130 interaction in gp130-mediated activities, and the contributions of gp130-activated MAPK and STAT signaling to PEL cell growth. Our data indicate that gp130 is essential for normal proliferation and viability of PEL cells and that ER-localized vIL-6/gp130-activated ERK and STAT3 signaling are critically important. These findings suggest that inhibitory targeting of vIL-6 interactions with the signal transducer within the ER may provide a useful strategy for PEL therapy or for targeting HHV-8 latency in normal B cells should vIL-6 be expressed in this latent reservoir.

MATERIALS AND METHODS

Cell culture, transfections, and lentivirus production. BCBL-1, JSC-1, BC-1, and BC-3 PEL cells and BJAB cells were maintained in RPMI 1640 medium supplemented with 10% heat-inactivated fetal bovine serum (FBS) and gentamicin. HEK293T cells were maintained in Dulbecco's modified Eagle's medium supplemented with 10% FBS and gentamicin. For transfections, HEK293T cells were passaged and plated at approximately 50% confluence, and these subconfluent monolayers were transfected with plasmids by standard calcium-phosphate-DNA coprecipitation. Cells were harvested 24 to 48 h posttransfection. Cell lysates were prepared by resuspending cells in lysis buffer (20 mM Tris [pH 8], 5 mM EDTA, 50 mM NaCl, 0.2% NP-40, 1× protease and phosphatase inhibitor cocktails [Sigma, St. Louis, MO; catalog numbers P8340 and P5726]), incubating suspensions on ice for 30 min, and centrifuging them (12,000 rpm for 5 min in a microcentrifuge) to remove cellular debris. Lysates were analyzed directly or stored at -20°C prior to Western blot analysis. Lentivirus was produced by transfecting HEK293T cells with short hairpin RNA (shRNA)-, vIL-6-, or sgp130-encoding or empty lentivirus plasmids (pYNC352 and pDUET001) together with gag/pol and vesicular stomatitis virus G protein expression vectors as previously described (22). Two days posttransfection, cell media were harvested, filtered, and centrifuged at $49,000 \times g$ to pellet virus. Viral pellets were resuspended in RPMI 1640 medium supplemented with 10% FBS, and aliquots were stored at -80°C . Infectious titers were established by using green fluorescent protein (GFP)-based or immunofluorescence microscopy to identify vector-transduced cells in PEL cell and other cultures prior to the experimental use of lentiviral vectors. For vIL-6 “rescue” experiments, PEL cells were first transduced with pYNC419-vIL-6.KDEL or pYNC419-vIL-6.W₁₆₇G.KDEL, allowed to recover for 5 days, selected in puromycin (1.0 $\mu\text{g}/\text{ml}$) for 2 weeks, and then transduced with either nonsilencing (NS) or vIL-6-specific shRNA encoded by pYNC352-derived lentiviruses. Cells transduced with shRNA or sgp130 were allowed to recover for 2 days prior to the normalization of cell numbers for growth assays.

Oligonucleotides and plasmids. shRNAs were chosen or designed to selectively deplete gp130, STAT1, STAT3, ERK1, or ERK2. Complementary oligonucleotides encoding 19-nucleotide short hairpin regions were annealed, phosphorylated, and cloned into the BamHI and MluI sites of the pYNC352 lentiviral vector. The following, prevalidated shRNA sequences were used: STAT1, GCGTAATCTTCAGGATAAT (23); STAT3, CATCTGCCTAGATCGGCTA (23, 24); used independently or together with AGTCAGGTTGCTGGTCAAA [23]); ERK1, GCCATGAGAGATGTCTACA (25); ERK2, GAGGATTGAAGTAGAACAG (25). The following shRNA sequences were designed and tested for gp130 depletion: GTGGGATCACCTATGAAGA (sh1), CTGTCCAAGACCTTAAACC (sh2), and TGCCCTTGGGAAGGTTACA (sh3). sh1 was used in subsequent functional analyses, alone or together with sh3. vIL-6 shRNA oligonucleotides and NS control shRNAs were described previously (8). For generation of

a lentiviral vector expressing KDEL motif-tagged vIL-6 variant W₁₆₇G (26), the corresponding vIL-6 coding sequences were first cloned between the BamHI and SmaI sites of pSG5.KDEL (26) to generate contiguous vIL-6.W₁₆₇G-KDEL coding sequences, and then these sequences were PCR amplified and inserted between the NotI and XhoI sites of pTYB6-derived lentiviral vector pYNC419 (26, 27). Lentiviral vector-cloned vIL-6 and vIL-6-KDEL and pSG5-cloned vIL-6, vIL-6-KDEL, vIL-6.W₁₆₇G, hIL-6, hIL-6-KDEL, gp130-Fc, and chitin binding domain (CBD)-fused VKORC1v2 have been described previously (8, 10, 22, 26, 28). The soluble gp130 (sgp130) expression vector was made by amplifying the first 972 nucleotides of gp130 (encoding domains 1 to 3) and inserting this sequence between the EcoRI and BamHI sites within the pSG5.KDEL vector, generating pSG5-sgp130.KDEL. A sequence encoding the FLAG epitope was then inserted at the BamHI site by using appropriate complementary oligonucleotides, generating pSG5-sgp130.FLAG.KDEL. The sgp130.FLAG.KDEL coding region was then amplified and ligated into the pDUET001 lentiviral vector (29) between the BamHI and XhoI sites. The integrity of all constructions was verified by sequencing.

Immunoblotting and coprecipitation assays. For Western blotting, heat-denatured and reduced proteins in cell lysate samples were size fractionated by sodium dodecyl sulfate-polyacrylamide gel electrophoresis (SDS-PAGE) and electrophoretically transferred to nitrocellulose membranes by standard procedures. Membranes were blocked with 5% nonfat milk in TBS-T (50 mM Tris-HCl [pH 7.4], 150 mM NaCl, 0.1% Tween 20), probed with primary antibodies (0.1 to 1.0 $\mu\text{g}/\text{ml}$) overnight at 4°C , washed in TBS-T buffer, and incubated with appropriate horseradish peroxidase-conjugated secondary antibodies in 5% TBS-T containing 5% nonfat milk. Blots were washed in TBS-T prior to visualization by standard chemiluminescence assay. For coprecipitation assays, cell lysates (prepared as described above) were added to either chitin beads (for precipitation of VKORC1v2-CBD) or protein A-agarose beads (for precipitation of gp130-Fc) and incubated with continuous rotation overnight at 4°C . Beads were then washed three times with lysis buffer. SDS loading buffer (188 mM Tris-HCl [pH 6.8], 3% SDS, 30% glycerol, 0.01% bromophenol blue, 15% β -mercaptoethanol) was added to precipitated samples, and these were then boiled before SDS-PAGE. Untreated lysate samples were also separated by SDS-PAGE to provide controls for protein expression, extraction, and transfer to immunoblotting membranes.

Antibodies. Commercially available antibodies to the following were used for Western blotting: bromodeoxyuridine (BrdU; BD Biosciences, Rockville, MD; catalog number 558599); pSTAT3 and pSTAT1 (Cell Signaling Technology, Beverly, MA; catalog numbers 9131 and 9171); β -actin (Sigma, St. Louis, MO; catalog number A2228); pERK, ERK1, STAT3, phosphotyrosine, and gp130 (Santa Cruz Biotechnology, Santa Cruz, CA; catalog numbers sc-7383, sc-94, sc-482, sc-508, and sc-655); hIL-6 (R&D Systems, Minneapolis, MN; catalog number MAB-206); and CBD (New England BioLabs, Ipswich, MA; catalog number E8034S). Rabbit antiserum to vIL-6 was generated in our laboratory and reported previously (26). The gp130 (BD Biosciences, Rockville, MD; catalog number 555756) and FLAG (Sigma, St. Louis, MO; catalog number F1804) primary antibodies and the Alexa Fluor 594 donkey anti-mouse IgG (H+L) secondary antibody (Invitrogen, Carlsbad, CA; catalog number A21203) were used for immunofluorescence staining.

Apoptosis and proliferation assays. Apoptosis was assessed via annexin V-Cy3 staining of cells. Briefly, cells were washed with phosphate-buffered saline (PBS) and resuspended in annexin V binding buffer (10 mM HEPES [pH 7.4], 140 mM NaCl, 2.5 mM CaCl_2) containing 0.4 μl of stock annexin V-Cy3 (BioVision, Mountain View, CA; catalog number 1002-200) per ml of binding buffer. Following incubation at room temperature in the dark for 5 min, cells were pelleted and washed with fresh binding buffer. Washed cell pellets were resuspended in 4% paraformaldehyde and fixed at room temperature for 20 min. Fixed cells were plated on glass slides and permeabilized with 0.25% Triton X-100 in PBS, and nuclei were stained with 4',6'-diamidino-2-phenylindole (DAPI) prior to

visualization. Several fields were used to calculate the percentage of annexin V-Cy3-positive cells in the total DAPI⁺ cell population. Cell proliferation rates were determined by BrdU incorporation assay. BrdU (10 μ M in RPMI 1640 medium supplemented with 10% FBS and gentamicin) was added to cell cultures that were then incubated for 2 h. Following incubation, the cells were washed in PBS, plated on glass slides, and allowed to dry. Cells were fixed in ice-cold methanol, washed in PBS, and incubated in 2 M HCl for 20 min at room temperature. HCl was neutralized with 0.1 M Na₂B₄O₇ (pH 8.5) for 2 min at room temperature. Slides were washed in PBS for 5 min and then washed three times for 10 min each in PBS containing 3% bovine serum albumin prior to incubation with Alexa Fluor 488-conjugated anti-BrdU antibody for 1 h at 37°C. Following PBS washing (three times, 5 min each), cells were stained with DAPI. Slides were visualized by UV microscopy to assess the percentage of BrdU-positive cells in the total cell population (DAPI⁺).

RESULTS

Contributions of gp130 to PEL cell growth. In previous studies, we found that depletion of vIL-6 in BCBL-1 and JSC-1 PEL cells led to autocrine-activity-mediated reductions in cell proliferation and survival and that ER-localized vIL-6 activity was sufficient for these functions (8). Subsequently, we determined that expression of VKORC1v2 and its interaction with vIL-6 were important gp130-independent contributors to the progrowth and antiapoptotic activities of vIL-6 in these cells (22). However, the possibility remained that vIL-6 signaling through gp130, in the ER and/or at the cell surface, also contributes to the effects of vIL-6 on PEL cells. The potential contribution of gp130 to PEL cell growth was tested by using lentivirus-delivered gp130-specific shRNA to deplete the endogenous expression of the signal transducer. Three shRNAs for gp130 depletion were designed (see Materials and Methods) and tested in lentivirus shRNA vector-transfected HEK293T cells, and each significantly depleted overexpressed gp130 levels relative to the vector-expressed gp130 levels observed in NS shRNA-transfected control cultures (data not shown). Two of these gp130 shRNA-expressing lentivirus vectors were used for single or dual transduction (see Materials and Methods) for subsequent experiments with PEL cells. The control NS shRNA-encoding lentiviral vector was used for comparison. Equivalent inoculating doses of lentiviruses were used, sufficient to provide ~90% transduction efficiency, as determined by lentivirus-expressed GFP fluorescence. After a postinfection incubation period of 2 days, the growth of cell density-normalized PEL cell cultures was monitored for an additional 3 days. For all of the PEL cell lines tested (BCBL-1, JSC-1, BC-1, and BC-3), gp130-targeted shRNAs led to significantly reduced cell growth relative to that of NS shRNA-transduced controls (Fig. 1A). Potential off-target, generally cytotoxic effects of gp130-directed shRNA were controlled for by equivalent experiments with HHV-8-negative BJAB cells, which were essentially unaffected by gp130 shRNA transduction relative to NS shRNA-transduced controls.

The observed reductions in PEL cell growth following gp130 depletion could be due to decreased cell survival and/or decreased rates of proliferation. This was investigated by using annexin V-Cy3 staining assays to detect apoptotic cells and BrdU incorporation analysis to identify S-phase cells in BCBL-1 and JSC-1 cultures transduced with either NS or gp130-specific shRNA. The data from these experiments revealed a correlation between gp130 depletion and both increased rates of apoptosis (Fig. 1B) and decreased rates of DNA synthesis (Fig. 1C). The combined results

indicate that gp130 signaling supports PEL cell growth by promoting both cell proliferation and cell survival.

Influence of gp130 on STAT and ERK signaling in PEL cells.

Signal transduction by gp130 involves activation of STAT and MAPK signaling. This proceeds via JAK-mediated tyrosine phosphorylation of gp130-recruited STAT1 and STAT3 and tyrosine and threonine phosphorylation of ERKs 1 and 2 following the activation of the MAPK signaling cascade, which is triggered by JAK phosphorylation of gp130-associating SHP2 (15). Active STAT3 has been reported previously to be expressed at constitutively high levels in PEL cells and to be important for PEL cell viability in culture (20). However, the mechanism of constitutive STAT3 activation in PEL cells and the biological significance of ERK signaling in these cells are unknown. To address the role of gp130 in the activation of STAT3 and ERK in the context of PEL cells, we again used gp130 depletion via lentiviral vector-mediated shRNA transduction. Targeting of gp130 resulted in detectably reduced levels of phospho-STAT3 (pSTAT3, active) and pSTAT1 in JSC-1, BCBL-1, BC-1, and BC-3 cells (Fig. 2A and B) and a marked decrease in phospho-ERK (pERK) levels in BCBL-1 and BC-1 cells but not in JSC-1 and BC-3 cells (Fig. 2C). The data from these experiments identify, for the first time, the contribution of gp130 to constitutively high pSTAT3 and pSTAT1 levels in PEL cells and provide evidence that gp130 can significantly influence ERK signaling in at least some PEL cell types (shown here for BCBL-1 and BC-1).

Contributions of STATs to PEL cell growth. It has been reported by others that STAT3 is essential for the viability of PEL cells (BC-1, BCBL-1, and VG-1) and that this activity involves STAT3-mediated induction of caspase-inhibitory and antiapoptotic protein survivin (20). These studies used transduced dominant negative STAT3 and the JAK pharmacological inhibitor AG490 to suppress levels of pSTAT3. Others have documented the importance of JAK-mediated, STAT-activating signaling in several PEL cell lines via the experimental use of JAK1-inhibitory curcumin; this was found to inhibit cell proliferation, promote apoptosis, and suppress inhibitor-of-apoptosis family proteins, including survivin (30). To independently assess the role of STAT3 in PEL cell growth, the transcription factor was targeted for depletion by shRNA-encoding lentiviruses. Two previously reported STAT3-targeted shRNAs (23, 24) were first tested in transfected HEK293T cells and verified as effective (data not shown). These shRNAs were each cloned into a lentiviral vector for introduction into PEL cells. Initial experiments indicated that single shRNA transduction was insufficient to achieve strong STAT3 depletion in PEL cell cultures, whereas coinfection of PEL cells with both lentiviral vectors was effective. For growth assays, BCBL-1 and JSC-1 cells were simultaneously infected with both STAT3-targeting lentiviral vectors or with an equivalent infectious dose of NS shRNA-encoding control lentivirus. The growth of posttransduction cell cultures was monitored by daily counting of trypan blue-excluding (viable) cells to determine cell densities (Fig. 3A). Suppression of STAT3 relative to levels in NS shRNA-transduced cultures was verified in terminal (day 3) cultures by Western blotting of cell extracts (Fig. 3A, right panels). The data revealed that STAT3 depletion substantially diminished the growth of these PEL cells, consistent with previously published studies (20), and identified JSC-1 PEL cells (not previously examined) as dependent on STAT3 for normal growth.

Further analyses were undertaken to test the contributions of

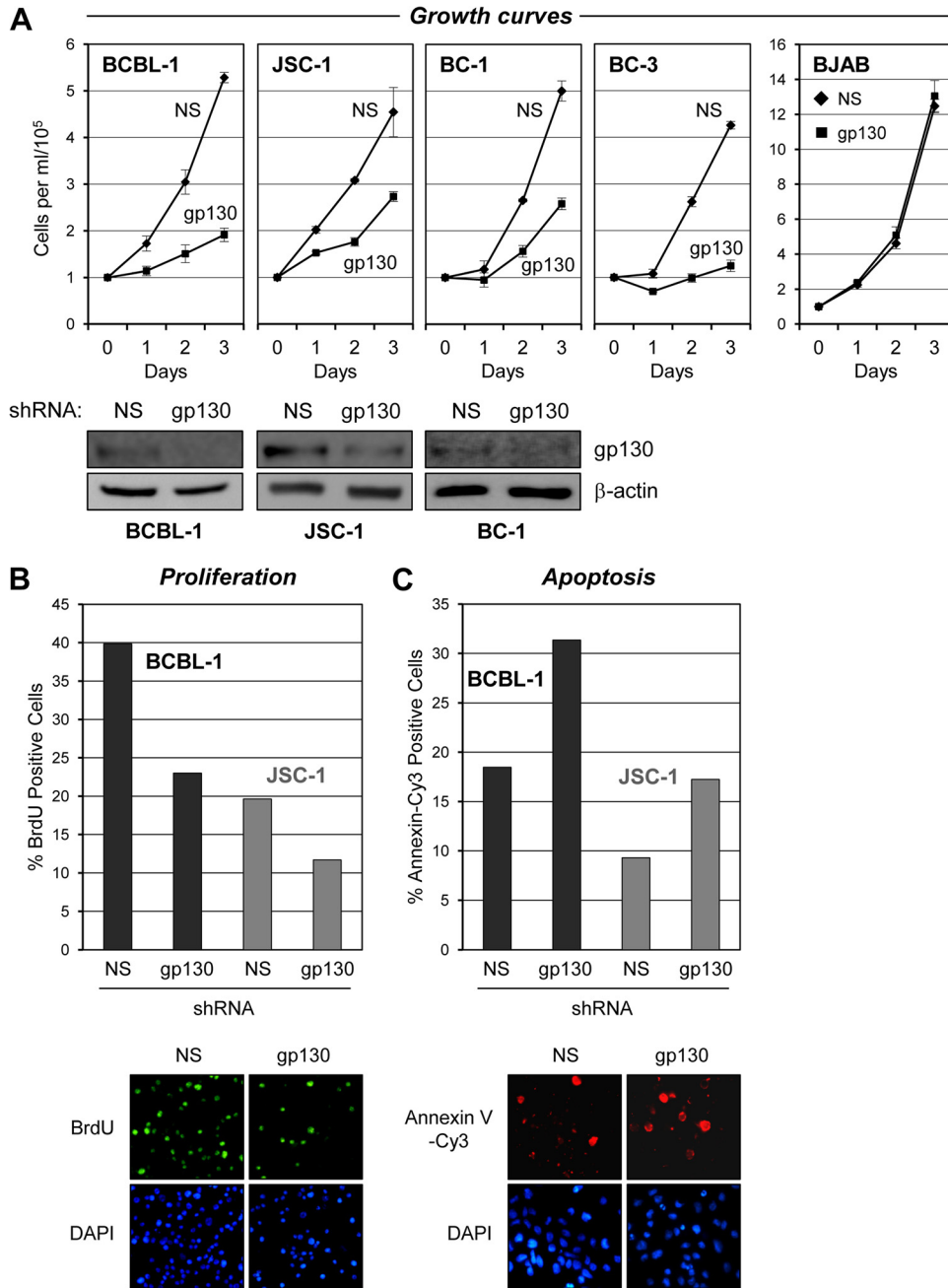


FIG 1 Effects of gp130 depletion on PEL cell growth and viability. (A) BCBL-1, JSC-1, BC-1, and BC-3 PEL cells and HHV-8-negative BJAB B cells were transduced either singly (BCBL-1, JSC-1, and BJAB) or dually (BC-1 and BC-3) with gp130-directed shRNA(s) by lentiviral infection (see Materials and Methods). Appropriate high-efficiency infection with the GFP-positive lentiviral vectors was evidenced by >90% GFP fluorescence in the cultures, which was sustained over the course of the 3-day growth experiment. Cell growth assays were initiated following cell density normalization and seeding of cells into fresh medium 48 h after lentiviral infection. Growth of the cultures was quantified by daily counting of trypan blue-excluding (viable) cells per ml with a hemocytometer. Cultures transduced with equivalent titers of a lentiviral vector expressing NS shRNA were used as controls. Triplicate cultures were infected with lentiviral vectors and monitored for growth. Error bars represent divergence from mean values determined for the triplicate cultures. Western blotting of cell lysates derived from pooled cultures at the end of the growth experiment (on day 3) was carried out to verify gp130 depletion; the respective blots are shown below the associated growth curves. For BC-3 cells, complete cytostatic effects of gp130 shRNA transduction resulted in insufficient cell numbers to process for immunoblotting. Levels of gp130 in BJAB cell lysates were below the limit of detection; the growth data show a lack of general cytostatic effects of lentivirus-mediated gp130 shRNA transduction. (B) Samples of gp130 and NS shRNA-transduced BCBL-1 and JSC-1 cultures harvested on day 2 from the growth curve experiments shown in panel A were analyzed for proliferation. Rates of proliferation were determined by detection of BrdU incorporation over a 2-h period into newly synthesized DNA with Alexa Fluor 488-conjugated, BrdU-specific antibody for immunofluorescence visualization of S-phase cells and counterstaining with DAPI to detect all nuclei. Relative proliferation rates are shown as the percentages of cells in S phase (BrdU positive) in the respective cultures. Data were derived from two random fields (>100 cells/field) of each slide-spotted culture sample. Examples of BrdU and DAPI costaining (sections of a single field, BCBL-1 cells) are shown below the quantified data. (C) Rates of apoptosis in these same PEL cell cultures were determined by annexin V-Cy3 binding. DAPI staining was again used to visualize nuclei, enabling calculation of the percentage of cells undergoing apoptosis. Examples of annexin V-Cy3 and DAPI costaining (of JSC-1 cells) are shown below the graphs. Cells were harvested on day 3 for the apoptosis assays.

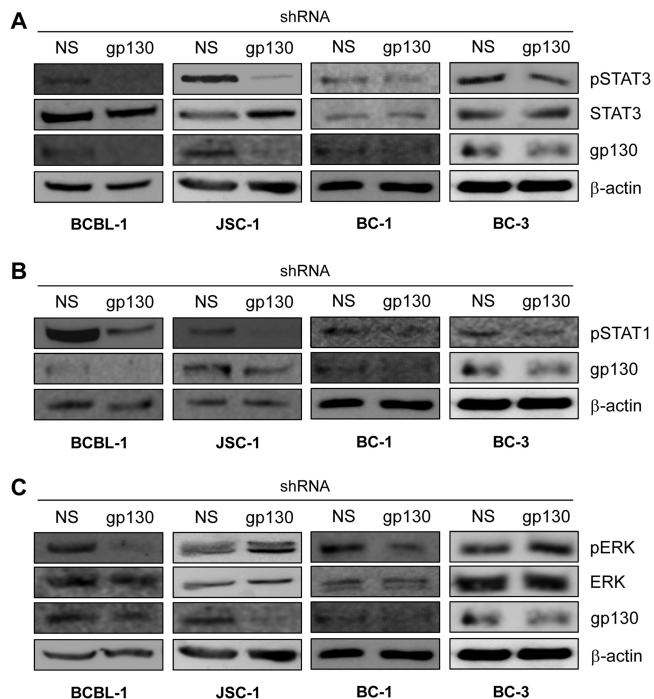


FIG 2 Contribution of gp130 signaling to levels of active STATs and ERKs in PEL cells. Phosphotyrosine-specific antibodies were used in immunoblotting to detect and determine the levels of phosphorylated (active), gp130-targeted STAT3 (A), STAT1 (B), and ERKs 1 and 2 (C) (pSTAT3, pSTAT1, and pERK) present in lysates of PEL cells depleted of gp130 relative to the levels of these proteins in NS shRNA-transduced controls. Antibodies detecting total (phosphorylated and unphosphorylated) STAT3 and ERK1/2 and β -actin were used to verify equivalent protein loading on SDS-PAGE gels and transfer to blotting membranes. For each set of lysates (used for single- or multiple-phosphoprotein detection), effective depletion of endogenous gp130 in the lentiviral shRNA-infected PEL cell cultures was verified by immunoblotting for gp130. Monitoring of growth of NS shRNA- versus gp130 shRNA-transduced cultures for BCBL-1, JSC-1, and BC-1 cells over 3 days (as described in the legend to Fig. 1) confirmed the growth-inhibitory effects of gp130 depletion (data not shown); cells were harvested on day 3 for Western analyses. For BC-3 cultures, all cells were harvested 48 h after lentiviral infection (day 0) to ensure sufficient material for immunoblotting.

STAT3 to the proliferation and survival of BCBL-1 and JSC-1 cells. These experiments involved immunofluorescence detection of BrdU incorporation and annexin V-Cy3 staining, respectively, as outlined above for the equivalent studies following gp130 depletion. Cells were harvested 5 days following lentiviral transduction (3 days postnormalization and culture) for BrdU and annexin V analyses. The results mirrored the effects of gp130 depletion, demonstrating that STAT3 depletion inhibited cell proliferation (proportion of cells in S phase) (Fig. 3B) and increased the rate of apoptosis (Fig. 3C). Thus, both of these components of cell biology are influenced by STAT3, which is activated by gp130 in these PEL cell lines.

As gp130 signaling involves the activation of STAT1 in addition to STAT3, we also explored the potential contribution of STAT1 activity to BCBL-1 and JSC-1 cell growth. Lentivirus-delivered shRNA (23) was used to deplete STAT1 in the respective cultures, and cell growth was compared to that of control (NS) shRNA-transduced cultures. The data revealed no significant effects of STAT1 depletion on BCBL-1 or JSC-1 cell growth, despite the achievement of robust depletion of pSTAT1 in BCBL-1 cells

and a nearly 2-fold reduction of pSTAT1 in JSC-1 cells, as demonstrated by Western blotting of terminal culture extracts (Fig. 3D). Although STAT1 depletion was somewhat limited in JSC-1 cells, these data suggest that STAT1 activity is not critical for PEL cell growth.

Contributions of ERKs 1 and 2 to PEL cell growth. As gp130 signaling involves the activation (phosphorylation) of ERKs 1 and 2 in addition to STATs, we undertook experiments to investigate the influence of ERK signaling on PEL cell growth. ERKs 1 and 2 were simultaneously targeted for depletion in BCBL-1 and JSC-1 cells by techniques analogous to those used for STAT depletion. The NS or ERK shRNA lentiviral vector-transduced cells were monitored for growth over a 3-day period by daily calculation of (trypan blue-excluding) cell densities in triplicate cultures of each cell type. In both PEL cell lines, ERK depletion led to dramatic reductions in cell growth relative to that of control (NS) shRNA-transduced cultures (Fig. 4A). Therefore, ERKs 1 and 2, in addition to STAT3, are essential for the normal growth of these cells.

The shRNA-transduced JSC-1 and BCBL-1 cultures were further analyzed to assess the effects of ERK depletion on cell proliferation and survival, specifically. Rates of proliferation and apoptosis in these cells following ERK1 and ERK2 depletion were examined by BrdU incorporation and annexin V-Cy3 staining, respectively, as outlined above. These analyses revealed that both proliferation and cell survival were reduced appreciably (between 2- and 3-fold) by ERK depletion (Fig. 4B and C).

Analysis of the effects of ERK depletion in two additional PEL cell lines, BC-1 and BC-3, indicated the general importance of ERKs 1 and 2 for PEL cell growth (Fig. 4D). The effects were not as marked in these cell lines as they were in BCBL-1 and JSC-1 cells, but it is possible that this was due to reduced efficacy of ERK depletion (Fig. 4D, bottom panels). In contrast, ERK depletion in the HHV-8-negative BJAB B cell line, reported previously to be insensitive to inhibition of ERK kinase (MEK) by PD98059 (31), had no effect on cell growth, verifying lack of general cytotoxic effects of lentiviral infection and ERK shRNA transduction (Fig. 4D, right). Combined, the data from our ERK depletion studies reveal the importance of ERK signaling, sustained in part via gp130 signal transduction in at least some PEL cell lines (BCBL-1 and BC-1, shown here), for PEL cell growth and viability.

ER-localized gp130-vIL-6 interaction contributes to vIL-6 and gp130 activities. We have previously reported that ER-localized vIL-6 and its interaction with the ER protein VKORC1v2 are important for PEL cell proliferation and viability (22). A previously characterized vIL-6 variant, vIL-6.W₁₆₇G, was used to determine the contribution of ER-localized vIL-6-gp130 interactions to PEL cell growth and survival. This altered vIL-6 protein is mutated in a region (site III) that interacts with gp130 domain 1 and is unable to induce dimerization of gp130 absent gp80 coexpression and hexameric complexing (12, 26). As ER-localized vIL-6 signaling occurs exclusively through tetrameric (vIL-6₂-gp130₂) complexes (8), vIL-6.W₁₆₇G should be unable to induce gp130 dimerization and signaling from the ER compartment. We first verified that ER-retained, KDEL motif-tagged vIL-6.W₁₆₇G was unable to induce gp130-mediated signaling in transfected HEK293T cells. Unlike wild-type vIL-6-KDEL, vIL-6.W₁₆₇G-KDEL was unable to induce tyrosine phosphorylation of gp130 or STAT3 (Fig. 5A). Coprecipitation assays with transfected cell lysates confirmed that the W₁₆₇G mutation did not affect the interaction between vIL-6 and VKORC1v2, which was tagged with

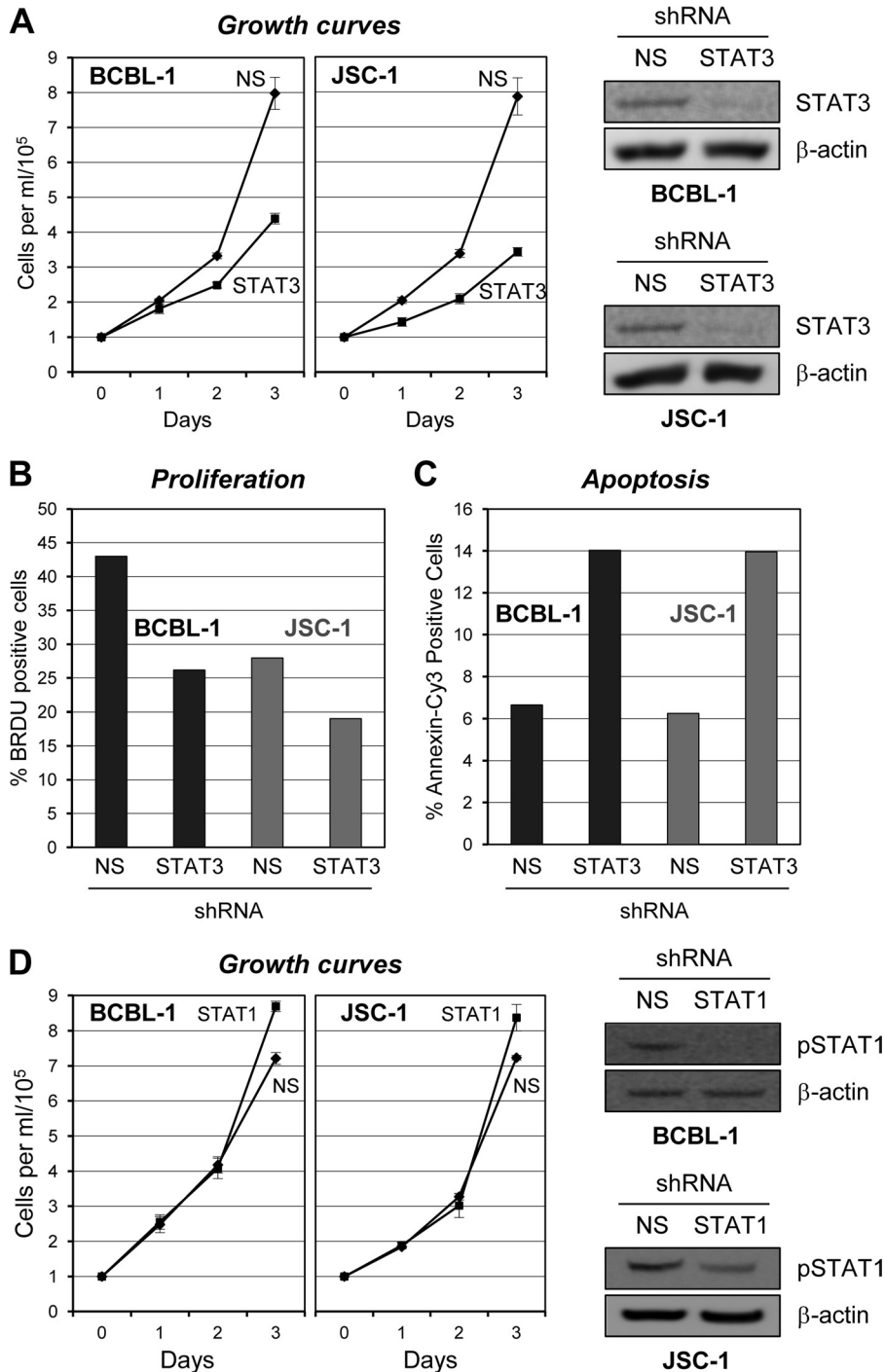


FIG 3 Contributions of gp130-activated STATs to PEL cell growth. (A) Appropriate lentiviral shRNA vectors (see Materials and Methods) were used in combination to infect BCBL-1 and JSC-1 PEL cells to deplete STAT3. Control cultures were infected with an equivalent dose of lentivirus encoding NS shRNA. Efficient lentiviral transduction of the respective cultures was verified by UV microscopy for the detection of lentiviral vector-expressed GFP; >90% of the cells in each culture were transduced with the STAT3-directed or NS shRNA-expressing vectors. Cells were allowed to rest for 2 days posttransduction, normalized to a cell density of 10⁵/ml, and monitored for cell growth as outlined in the Fig. 1 legend. Growth curves were derived from triplicate cultures transduced separately with the NS and STAT3-targeting lentiviral shRNA vectors and monitored in parallel. Error bars represent deviations from the mean cell density at each 24-h time point over the 3-day experiment. Pooled cultures were harvested at the end of the experiment (day 3) for Western analysis of cell lysates to check for depletion of STAT3. (B) Proliferation of STAT3-depleted versus NS shRNA-transduced BCBL-1 and JSC-1 cells was examined by BrdU incorporation assay of cells harvested on day 3 (5 days after shRNA transduction) as outlined in the legend to Fig. 1. (C) Rates of apoptosis in these same culture samples were determined by annexin V-Cy3 binding assays and costaining of cell nuclei with DAPI (see above, Fig. 1 legend). (D) STAT1 depletion experiments were performed to examine the potential contributions of STAT1 to BCBL-1 and JSC-1 cell growth. STAT1 depletion was mediated by infection of PEL cell cultures with a lentiviral vector encoding a STAT1 mRNA-targeting shRNA (see Materials and Methods), and NS shRNA-encoding lentivirus was used as a control as before. While substantial depletion of STAT1 was apparent for each cell line (immunoblots, right), the growth of neither was altered significantly as a result. Chemiluminescence signals in Western blot assays were digitally captured, quantified with imager-associated software, and normalized to the β-actin signal. The pSTAT1 levels in JSC-1 cultures were 1.9-fold lower than those in the corresponding NS shRNA-transduced controls; no pSTAT1-specific signal was detected in BCBL-1 cell lysates from STAT1 shRNA-transduced cultures.

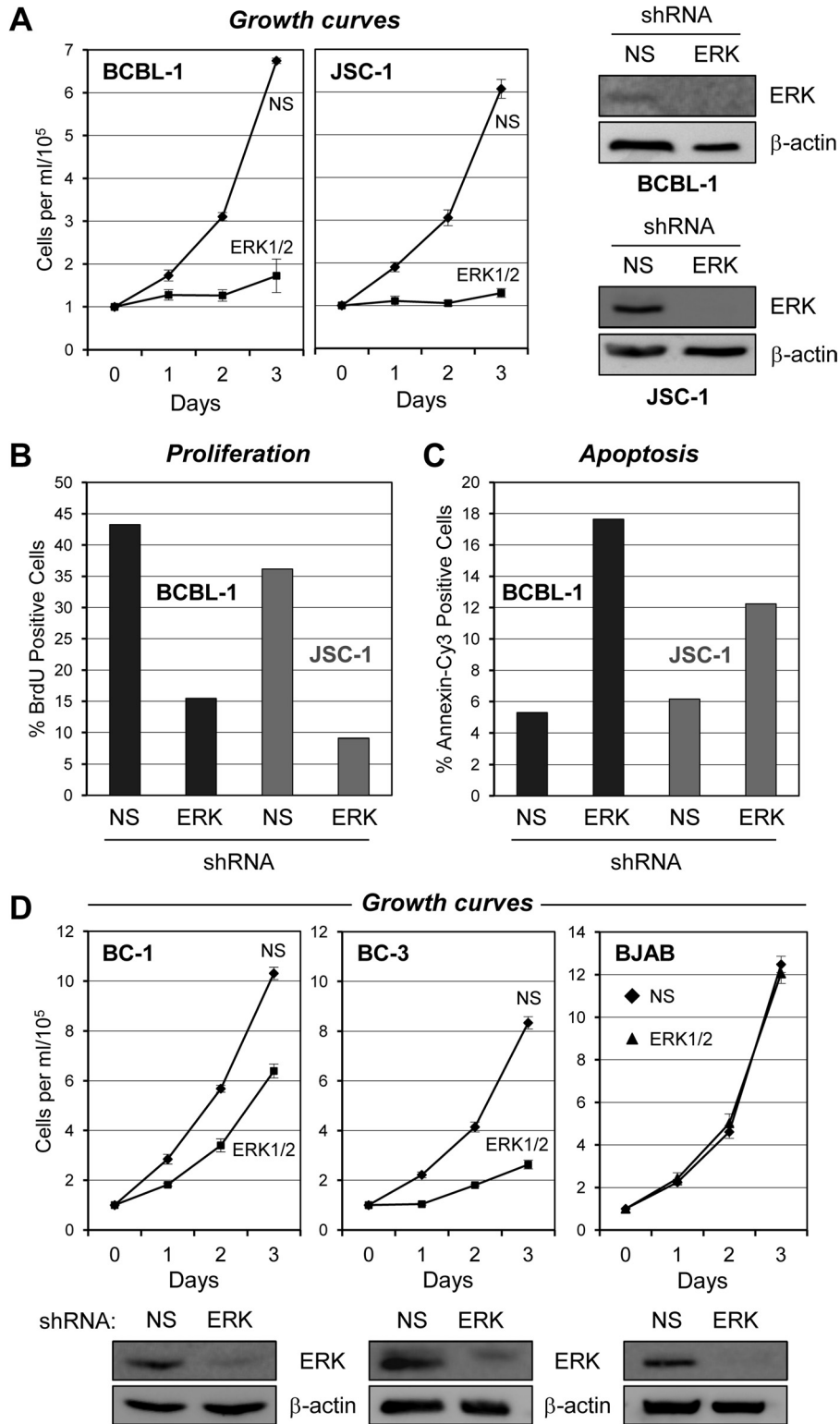


FIG 4 Analysis of culture growth, cell proliferation, and apoptosis rates as a function of ERK depletion. (A) Potential contributions of ERK to the growth of BCBL-1 and JSC-1 cultures were examined by monitoring the growth of cells transduced with lentiviral vectors encoding either ERK-targeting or NS (control) shRNAs. Cell samples were harvested at 24-h intervals following posttransduction normalization (day 0). Error bars indicate deviations from average values derived from triplicate cultures. Effective ERK depletion was verified by immunoblotting of lysates from BCBL-1 and JSC-1 cells pooled from the respective triplicate cultures and harvested at the end of the experiment. β-Actin was used as a control for equivalent protein loading and membrane transfer. (B) Relative proliferation rates of BCBL-1 and JSC-1 cultures transduced with NS or ERK1/2-directed shRNA were determined by BrdU incorporation assay (see Materials and Methods). Cells were harvested 4 days after shRNA transduction and 2 days postnormalization prior to growth monitoring (A). Visualization of DNA-incorporated BrdU was mediated by appropriate immunostaining; counterstaining with DAPI enabled covisualization of all cell nuclei. The proportions

CBD to facilitate precipitation and enable immune detection with a CBD-specific antibody (Fig. 5B). KDEL-tagged, shRNA-resistant versions of wild-type and $W_{167}G$ -mutated vIL-6 were then used to supplement vIL-6-depleted PEL cells to determine if the gp130 dimerization-defective but VKORC1v2 binding-competent variant could rescue cell growth. These experiments were analogous to those undertaken previously with vIL-6-KDEL, which demonstrated sufficiency of ER-localized vIL-6 for maintenance of BCBL-1 and JSC-1 cell growth and viability (8). In contrast to vIL-6-KDEL, vIL-6. $W_{167}G$ -KDEL was unable to complement endogenous vIL-6 depletion (Fig. 5C), indicating that vIL-6-induced dimerization of gp130 and its downstream signaling are critically important for the proproliferative activity of ER-localized vIL-6 in PEL cells.

The importance of intracellular gp130 signaling was further tested by using lentivirus-transduced sgp130, which was KDEL motif fused for ER retention. Initial experiments using transfected HEK293T cells were undertaken to verify the ability of this protein to inhibit ER-localized (vIL-6.KDEL), but not extracellular (hIL-6), signal transduction via endogenously expressed gp130 (Fig. 6A). Additionally, the intracellular localization of sgp130.KDEL (FLAG tagged) was tested and compared to the distribution of full-length gp130 by anti-FLAG and anti-gp130 antibody-based immunofluorescence assays of transfected cells; cells were cotransfected with GFP-KDEL, which provided an ER marker (8). In contrast to native gp130, sgp130.KDEL was present at high levels intracellularly with little, if any, surface fluorescence detectable (Fig. 6B). Having confirmed the expression and appropriate ER localization of lentiviral vector-expressed sgp130.KDEL, we then used this vector or an empty control vector to transduce PEL cells to determine the effects of ER-localized gp130 inhibition on cell growth and apoptosis. The data revealed significant effects of sgp130.KDEL on the growth of both BCBL-1 and JSC-1 cultures (Fig. 6C). BrdU incorporation assays using cells harvested at day 2 from the growth experiment confirmed the inhibition of proliferation (i.e., percentage of cells in S phase) by introduced sgp130.KDEL (Fig. 6D). In a separate experiment, transduction of sgp130.KDEL into BCBL-1 and JSC-1 cells led to substantial increases in the rates of apoptosis, as determined by annexin V-Cy3 staining (Fig. 6E). As vIL-6 is the only known cytokine to signal through gp130 from the ER compartment (and ER-retained hIL-6 has been demonstrated to be unable to do so [8]), these data suggest strongly that vIL-6-gp130 signaling is of biological significance and contributes, wholly or in part, to the progrowth and prosurvival effects of gp130 on these cells.

DISCUSSION

The work reported here addressed the contribution of gp130 signaling to the constitutively high levels of active STAT3 reported in PEL cells, the influence of gp130 activity on STAT1 and ERK ac-

tivation in these cells, and the functional relevance of vIL-6-mediated gp130 activity to PEL cell growth. To our knowledge, our data are the first to document a mechanism for the constitutively high levels of active STAT3 in PEL cells, to establish a critical role for the gp130 signal transducer in supporting PEL cell proliferation and viability, and to identify the relevance of gp130 targeting by vIL-6 to these activities. Thus, in addition to the important association of vIL-6 with VKORC1v2 for PEL cell growth and survival (8), the activity of the viral cytokine through its well-established signal transducer is also critical. This activity is mediated from the ER, where vIL-6 is predominantly localized. A VKORC1v2 binding-competent, gp130 dimerization-defective vIL-6 variant ($W_{167}G$) that was restricted to the ER was unable to rescue the effects of vIL-6 depletion, in contrast to KDEL motif-tagged wild-type vIL-6. Furthermore, ER-localized sgp130, used as a competitive inhibitor of gp130-vIL-6 interactions in the ER compartment, enabled the identification of the specific role of vIL-6 as a mediator of gp130 function in the context of PEL. Thus, gp130 and ER-localized vIL-6 signaling via gp130 have been shown for the first time to support PEL cell proliferation and viability. Therefore, gp130 and its interaction with vIL-6 have been identified as potential targets for therapeutic intervention.

Another important finding from this study is that ERK activation contributes significantly to the growth and survival of PEL cells. Depletion of ERK led to severe abrogation of cell proliferation (3-fold reductions in BrdU incorporation) and to greatly (2- to 3-fold) increased rates of apoptosis in BCBL-1 and JSC-1 cultures, effectively halting culture growth. Significant effects of ERK depletion on the growth of BC-1 and BC-3 cells were also identified. At least for BCBL-1 and BC-1 cells (included in this study), the high levels of active, tyrosine-phosphorylated ERK (pERK) are dependent on gp130. However, gp130 depletion did not diminish the levels of pERK in JSC-1 and BC-3 cells; pERK was actually increased in both cell lines. These patterns were observed in multiple repeat experiments with these PEL cell lines. In contrast to the effects of ERK depletion on PEL cell growth, ERK depletion in HHV-8-negative BJAB cells did not affect cell growth at all. The role of ERK signaling in HHV-8 biology has previously been noted only in connection with *de novo* infection, establishment of latency, and lytic reactivation. Thus, pharmacological inhibition of ERK activation suppresses TPA-induced lytic gene expression and replication in PEL cell cultures (32–35). Additionally, activation of ERK-targeting signaling pathways and their requirement for *de novo* infection, postentry lytic gene expression, and latency establishment have been reported in endothelial cell systems (34, 36, 37). Our results now add to this body of knowledge regarding the role of ERK signaling in HHV-8 biology by identifying ERK as an important factor in the maintenance of PEL cell viability and by establishing gp130 signaling as a mechanism contributing to high levels of active ERK in at least some PEL cell types.

of BrdU-positive S-phase cells are expressed as percentages of the total cell population (DAPI⁺) for BCBL-1 and JSC-1 cultures (dark and light bars, respectively). Data, expressed as averages, were derived from multiple random microscopic fields (>100 cells/field) of each culture. (C) Apoptosis in the same cultures (harvested 5 days posttransduction and on day 3 of counting) was identified by annexin V-Cy3 staining; data are expressed as percentages of the total DAPI⁺ population. Average values derived from multiple random microscopic fields are shown. (D) Growth experiments equivalent to those shown in panel A were undertaken to determine the effects of ERK depletion on two additional PEL cell lines, BC-1 and BC-3, in addition to HHV-8-negative BJAB cells, which were previously shown to be refractory to ERK kinase (MEK) inhibition (31) and used here as a control for potential nonspecific cytotoxic effects of ERK shRNA transduction. The growth of PEL cell lines, but not BJAB cultures, was inhibited by ERK shRNA transduction relative to that of NS shRNA-expressing controls. Effective ERK depletion in each of the three cell lines was verified by immunoblotting for ERKs 1 and 2; β -actin antibody was used to check for equal protein loading and membrane transfer. Blots of all of the cell lines are shown below the respective growth curves.

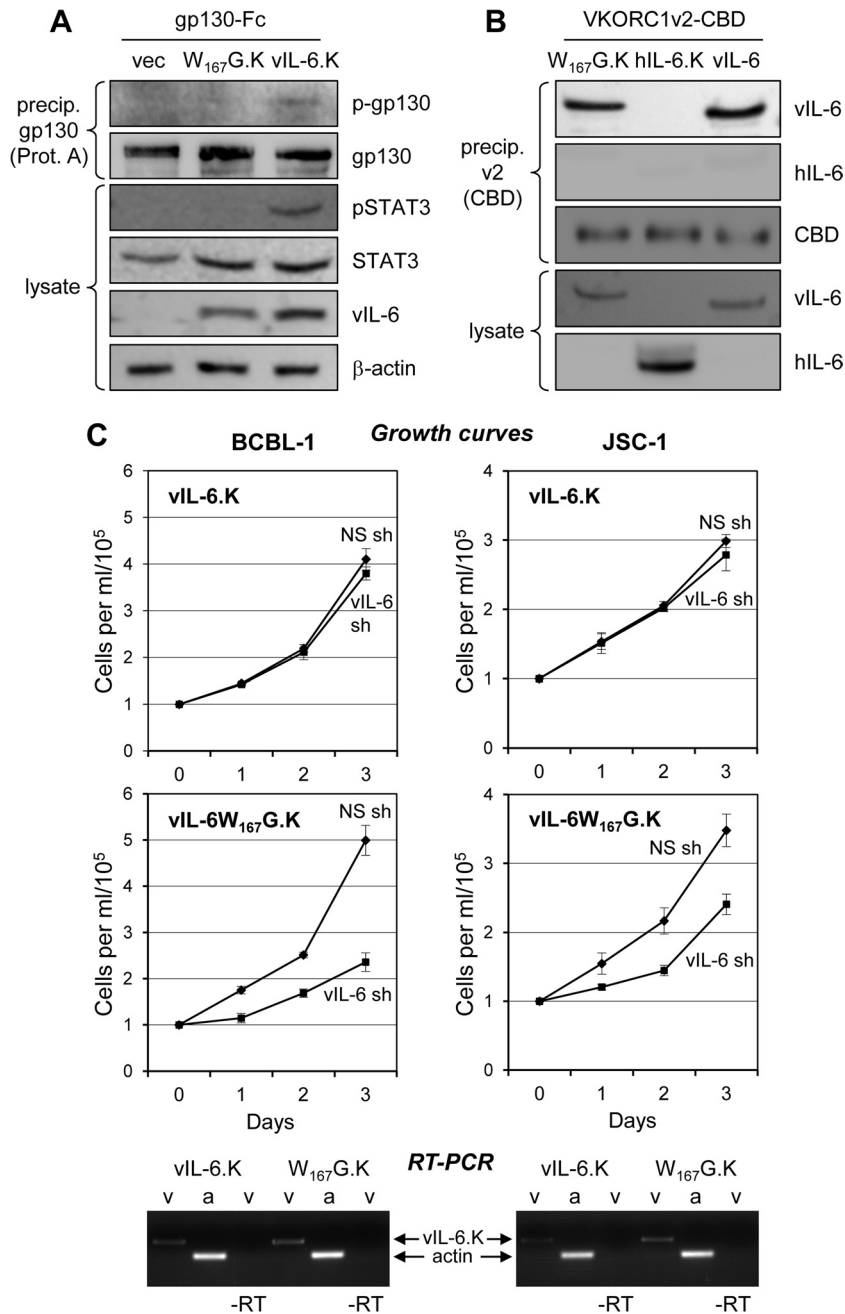


FIG 5 ER-localized vIL-6 signal transduction via gp130 supports PEL cell growth. (A) Previously described vIL-6 variant W₁₆₇G, which has a weakened interaction with gp130 domain 1 and cannot form tetrameric (vIL-6₂-gp130₂, ER-localized) complexes (12, 26), was tested in transfected HEK293T cells to verify its predicted inability to mediate signal transduction when restricted to the ER compartment. KDEL-tagged, ER-directed forms of vIL-6 and vIL-6.W₁₆₇G were expressed together with Fc-tagged gp130 from appropriate expression plasmids. After 24 h, cell lysates were analyzed by immunoblotting for pSTAT3, an indicator of gp130 signaling, and protein (Prot.) A-agarose-precipitated gp130-Fc was probed with phosphotyrosine-specific antibody for the detection of activated gp130. Only wild-type vIL-6 (vIL-6.K) was able to signal via gp130 in the ER compartment, inducing gp130 and STAT3 phosphorylation, in contrast to vIL-6.W₁₆₇G-KDEL (W₁₆₇G.K) and the empty vector (vec). (B) Testing of VKORC1v2 binding by vIL-6.W₁₆₇G was undertaken by coimmunoprecipitation assay, which was used previously for the detection of the vIL-6-VKORC1v2 interaction (22). CBD-tagged VKORC1v2 was precipitated (precip.) with chitin beads from lysates of transfected cells, and the precipitated material was analyzed by immunoblotting for the presence of vIL-6.W₁₆₇G-KDEL, wild-type vIL-6 (positive control), or KDEL motif-tagged hIL-6 (hIL-6.K, negative control) expressed in separately transfected cultures. Both vIL-6 proteins were precipitated and therefore competent for interaction with VKORC1v2; binding of VKORC1v2 by vIL-6.W₁₆₇G-KDEL verified that the site III mutation affected only gp130 binding. (C) Experiments with shRNA-mediated vIL-6 depletion and complementation with KDEL-tagged, ER-restricted vIL-6 (vIL-6.K) and vIL-6.W₁₆₇G (W₁₆₇G.K) were undertaken to determine whether vIL-6 signaling through ER-localized gp130 is important for PEL cell growth. BCBL-1 and JSC-1 cells were first transduced with a lentiviral vector expressing either vIL-6.K or vIL-6.W₁₆₇G.K (designed to be refractory to vIL-6 shRNA) and then transduced with a lentiviral vector expressing NS or vIL-6-directed shRNA. Triplicate cultures were monitored for growth as outlined above and in Materials and Methods; error bars indicate standard deviations from the mean cell density. Below the plots, ethidium bromide-stained agarose gels are shown containing reverse transcriptase (RT) PCR-amplified vIL-6 mRNA sequences extracted from lysates of PEL cell samples derived from the growth assay cultures. The data provide evidence of the appropriate and equivalent expression of each of the vIL-6 constructions. RT-PCR products amplified with PCR primer pairs for vIL-6.K (v) and β-actin (a), which was used as a normalization control, are indicated. Omission of RT (-RT) provided a control for RNA-derived vIL-6.K PCR products (i.e., lack of DNA contamination).

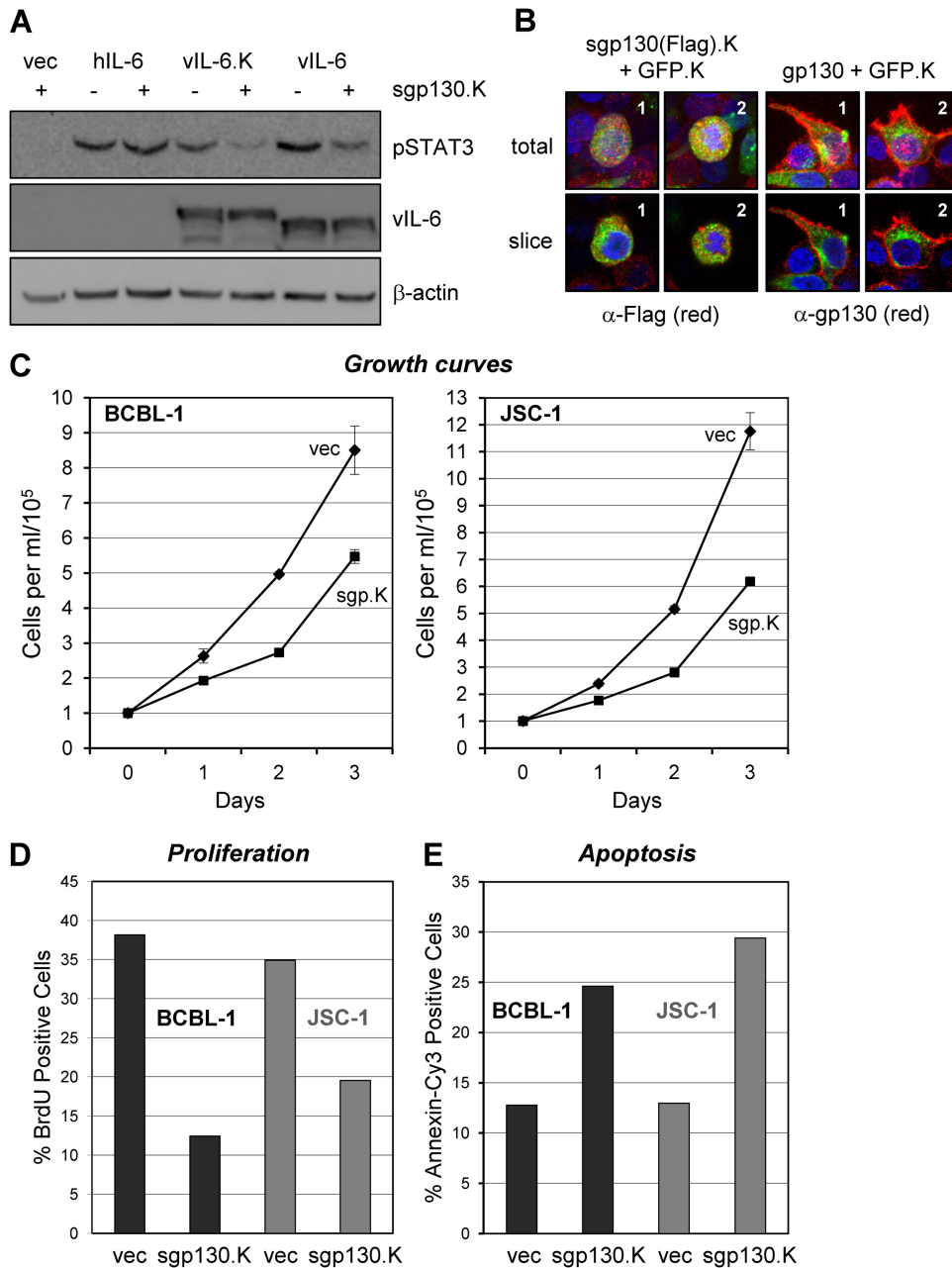


FIG 6 Inhibitory targeting of vIL-6/gp130 signaling diminishes PEL cell proliferation and survival. (A) Functional testing of KDEL motif-fused (ER-directed and retained) and FLAG epitope-tagged sgp130 (sgp130.K) as an inhibitor of ER-localized vIL-6 signaling in transfected HEK293T cells. Cultures were cotransfected with expression vectors for sgp130.K (or the empty-vector control, vec) and either vIL-6, vIL-6-KDEL (vIL-6.K), or hIL-6. Cells were harvested at 48 h posttransfection for preparation of cell lysates. These were analyzed by Western blotting for detection of pSTAT3, an indicator of gp130 signaling, and β -actin (protein loading control). vIL-6 (mainly ER localized but also secreted) and KDEL-tagged vIL-6 (completely ER retained [8]) signaling was inhibited by sgp130.K, whereas signaling by hIL-6 (efficiently secreted) was unaffected. The data verified the ER-restricted, vIL-6-gp130 inhibitory activity of sgp130.K. (B) Confirmation of intracellular localization of KDEL motif-fused and FLAG-tagged sgp130 and comparison to (surface-expressed) full-length gp130 via FLAG- and gp130-based immunofluorescence staining of transfected cells; Alexa Fluor 594-conjugated secondary antibody was used for (red) fluorescence signal detection. Each protein was expressed together with KDEL-tagged GFP (GFP.K, used previously as an ER marker [8]) in vector-cotransfected HEK293T cells. As expected, FLAG-specific staining for sgp130.FLAG.KDEL [sgp130(Flag).K] was evident intracellularly and was coincident with the ER-localized GFP signal, whereas gp130 staining was localized mainly to the cell surface. Stacked (total) and representative individual z sections (slice) are shown for two examples (1 and 2) taken from each of the transfected cultures. (C) BCBL-1 and JSC-1 cells were transduced with equivalent titers of the empty (vec) and sgp130-KDEL (sgp130.K)-expressing lentiviral vectors, and the growth of cell density-normalized cultures was monitored after a 2-day rest-and-recovery period. Densities of trypan blue-excluding (viable) cells in triplicate cultures were determined daily; error bars represent standard deviations from derived average values. (D) Relative proliferation rates of PEL cells at day 2 (from growth assays) were determined by 2-hr BrdU incorporation assays (see Materials and Methods). (E) In a separate experiment, transduction of sgp130.K into BCBL-1 and JSC-1 cultures led to induction of apoptosis, as determined by annexin V-Cy3 staining. Cells were harvested and analyzed 3 days posttransduction with test (sgp130.K) and control (vec) lentiviral vectors.

A previous study by Aoki and colleagues (20) demonstrated that the JAK inhibitor AG490 and ectopic expression of a dominant negative STAT3 protein (DNA binding refractory) led to dramatically reduced PEL cell viability. The PEL cell lines investigated were BCBL-1, BC-1, and VG-1. Our experiments investigating the role of STAT3 used BCBL-1 and JSC-1 cells, which were characterized in depth previously with respect to latent expression and progrowth and prosurvival activities of ER-localized vIL-6 (8). A caveat of the experiments using AG490 is that this pharmacological inhibitor can affect JAK-activated receptors other than gp130 and receptor-mediated activation of STATs other than STAT3; AG490 may also have nonspecific effects on other pathways. Of additional note is that experimental use of the STAT3 dominant negative protein, while very effective at blocking endogenous STAT3 activity, also has the potential to inhibit STAT1 and other STAT3-heterodimerizing proteins; thus, it may affect STAT3-independent mechanisms. However, the data previously reported by Aoki et al. (20), combined with our independently derived and concordant results from STAT3 depletion experiments, provide very strong evidence that STAT3 signaling is critical to PEL cell biology. STAT3 signaling was shown to induce the prosurvival protein survivin, which was found to be an important factor in STAT3-mediated prosurvival effects in PEL cells (20). However, it is noteworthy that the JAK-targeting STAT signaling inhibitor curcumin, while demonstrated in an independent study to induce cell death with concomitant suppression of survivin in most of the PEL cell lines tested, did not lead to a significant loss of survivin expression in BCBL-1 cells (used in the present study and that of Aoki et al. [20]) (30). Thus, survivin may not be the only STAT3-regulated factor critical to PEL cell viability. Nonetheless, our data reveal that gp130 and ER-localized vIL-6 activity through the signal transducer can contribute to high constitutive levels of active pSTAT3, a factor that has been linked to cell growth and survival in PEL and other neoplasias as well as under normal physiological conditions (18, 38, 39), and to promotion of cell proliferation and viability. It is noteworthy that gp130-dependent constitutively high levels of active STAT3 have also been detected in endothelial cells latently infected with HHV-8, although via (paracrine) mechanisms independent of vIL-6 (40). Furthermore, *de novo* infection of blood endothelial cells leads to STAT3 induction and gp130-dependent, but vIL-6-independent, lymphatic endothelial cell reprogramming (41). Thus, STAT3 signaling, in part mediated via gp130, may be generally important for maintenance of HHV-8 latency and viability of latently infected cells and may also contribute to virus-associated neoplasia.

In conclusion, the data presented here document for the first time the significance of gp130-mediated signaling for the proliferation and survival of PEL cells, the importance of gp130 as a contributor to constitutively high levels of functionally significant STAT and/or ERK signaling in at least some PEL cell lines, and the contribution of ER-localized vIL-6–gp130 interactions for PEL cell growth and viability. These data broaden our understanding of the role and mechanisms of action of latently expressed vIL-6 in PEL cell biology and provide further support for the idea that drug targeting of the viral cytokine and its signal transducer, within the ER compartment, may represent a useful therapeutic strategy.

ACKNOWLEDGMENTS

We thank Daming Chen and Gordon Sandford for scientific and technical advice and support.

This work was supported by NCI grant R01-CA76445 to J.N. and NIH Ruth Kirschstein Fellowship F31-CA171933 to E.C.

REFERENCES

1. Ensoli B, Sturzl M, Monini P. 2001. Reactivation and role of HHV-8 in Kaposi's sarcoma initiation. *Adv. Cancer Res.* **81**:161–200.
2. Schulz TF. 2006. The pleiotropic effects of Kaposi's sarcoma herpesvirus. *J. Pathol.* **208**:187–198.
3. Uldrick TS, Polizzotto MN, Yarchoan R. 2012. Recent advances in Kaposi sarcoma herpesvirus-associated multicentric Castlemans disease. *Curr. Opin. Oncol.* **24**:495–505.
4. Nicholas J. 2007. Human herpesvirus 8-encoded proteins with potential roles in virus-associated neoplasia. *Front. Biosci.* **12**:265–281.
5. Sakakibara S, Tosato G. 2011. Viral interleukin-6: role in Kaposi's sarcoma-associated herpesvirus: associated malignancies. *J. Interferon Cytokine Res.* **31**:791–801.
6. Jones KD, Aoki Y, Chang Y, Moore PS, Yarchoan R, Tosato G. 1999. Involvement of interleukin-10 (IL-10) and viral IL-6 in the spontaneous growth of Kaposi's sarcoma herpesvirus-associated infected primary effusion lymphoma cells. *Blood* **94**:2871–2879.
7. Chandriani S, Ganem D. 2010. Array-based transcript profiling and limiting-dilution reverse transcription-PCR analysis identify additional latent genes in Kaposi's sarcoma-associated herpesvirus. *J. Virol.* **84**:5565–5573.
8. Chen D, Sandford G, Nicholas J. 2009. Intracellular signaling mechanisms and activities of human herpesvirus 8 interleukin-6. *J. Virol.* **83**:722–733.
9. Molden J, Chang Y, You Y, Moore PS, Goldsmith MA. 1997. A Kaposi's sarcoma-associated herpesvirus-encoded cytokine homolog (vIL-6) activates signaling through the shared gp130 receptor subunit. *J. Biol. Chem.* **272**:19625–19631.
10. Chen D, Nicholas J. 2006. Structural requirements for gp80 independence of human herpesvirus 8 interleukin-6 (vIL-6) and evidence for gp80 stabilization of gp130 signaling complexes induced by vIL-6. *J. Virol.* **80**:9811–9821.
11. Adam N, Rabe B, Suthaus J, Grotzinger J, Rose-John S, Scheller J. 2009. Unraveling viral interleukin-6 binding to gp130 and activation of STAT-signaling pathways independently of the interleukin-6 receptor. *J. Virol.* **83**:5117–5126.
12. Boulanger MJ, Chow DC, Brevnova E, Martick M, Sandford G, Nicholas J, Garcia KC. 2004. Molecular mechanisms for viral mimicry of a human cytokine: activation of gp130 by HHV-8 interleukin-6. *J. Mol. Biol.* **335**:641–654.
13. Hu F, Nicholas J. 2006. Signal transduction by human herpesvirus 8 viral interleukin-6 (vIL-6) is modulated by the nonsignaling gp80 subunit of the IL-6 receptor complex and is distinct from signaling induced by human IL-6. *J. Virol.* **80**:10874–10878.
14. Meads MB, Medveczky PG. 2004. Kaposi's sarcoma-associated herpesvirus-encoded viral interleukin-6 is secreted and modified differently than human interleukin-6: evidence for a unique autocrine signaling mechanism. *J. Biol. Chem.* **279**:51793–51803.
15. Heinrich PC, Behrmann I, Muller-Newen G, Schaper F, Graeve L. 1998. Interleukin-6-type cytokine signalling through the gp130/Jak/STAT pathway. *Biochem. J.* **334**(Pt 2):297–314.
16. Kovaleva M, Bussmeyer I, Rabe B, Grotzinger J, Sudarman E, Eichler J, Conrad U, Rose-John S, Scheller J. 2006. Abrogation of viral interleukin-6 (vIL-6)-induced signaling by intracellular retention and neutralization of vIL-6 with an anti-vIL-6 single-chain antibody selected by phage display. *J. Virol.* **80**:8510–8520.
17. Benekli M, Baumann H, Wetzler M. 2009. Targeting signal transducer and activator of transcription signaling pathway in leukemias. *J. Clin. Oncol.* **27**:4422–4432.
18. Bowman T, Garcia R, Turkson J, Jove R. 2000. STATs in oncogenesis. *Oncogene* **19**:2474–2488.
19. Hodge DR, Hurt EM, Farrar WL. 2005. The role of IL-6 and STAT3 in inflammation and cancer. *Eur. J. Cancer* **41**:2502–2512.
20. Aoki Y, Feldman GM, Tosato G. 2003. Inhibition of STAT3 signaling induces apoptosis and decreases survivin expression in primary effusion lymphoma. *Blood* **101**:1535–1542.
21. Oldenburg J, Bevans CG, Muller CR, Watzka M. 2006. Vitamin K epoxide reductase complex subunit 1 (VKORC1): the key protein of the vitamin K cycle. *Antioxid. Redox Signal.* **8**:347–353.

22. Chen D, Cousins E, Sandford G, Nicholas J. 2012. Human herpesvirus 8 viral interleukin-6 interacts with splice variant 2 of vitamin K epoxide reductase complex subunit 1. *J. Virol.* **86**:1577–1588.
23. Ho HH, Ivashkiv LB. 2006. Role of STAT3 in type I interferon responses. Negative regulation of STAT1-dependent inflammatory gene activation. *J. Biol. Chem.* **281**:14111–14118.
24. Huang F, Tong X, Fu L, Zhang R. 2008. Knockdown of STAT3 by shRNA inhibits the growth of CAOV3 ovarian cancer cell line in vitro and in vivo. *Acta Biochim. Biophys. Sin. (Shanghai)* **40**:519–525.
25. Chatterjee M, Stuhmer T, Herrmann P, Bommert K, Dorken B, Bargou RC. 2004. Combined disruption of both the MEK/ERK and the IL-6R/STAT3 pathways is required to induce apoptosis of multiple myeloma cells in the presence of bone marrow stromal cells. *Blood* **104**:3712–3721.
26. Wan X, Wang H, Nicholas J. 1999. Human herpesvirus 8 interleukin-6 (vIL-6) signals through gp130 but has structural and receptor-binding properties distinct from those of human IL-6. *J. Virol.* **73**:8268–8278.
27. Chang LJ, Zaiss AK. 2003. Self-inactivating lentiviral vectors and a sensitive Cre-loxP reporter system. *Methods Mol. Med.* **76**:367–382.
28. Nicholas J, Ruvolo VR, Burns WH, Sandford G, Wan X, Ciufo D, Hendrickson SB, Guo HG, Hayward GS, Reitz MS. 1997. Kaposi's sarcoma-associated human herpesvirus-8 encodes homologues of macrophage inflammatory protein-1 and interleukin-6. *Nat. Med.* **3**:287–292.
29. Zhou BY, Ye Z, Chen G, Gao ZP, Zhang YA, Cheng L. 2007. Inducible and reversible transgene expression in human stem cells after efficient and stable gene transfer. *Stem Cells* **25**:779–789.
30. Uddin S, Hussain AR, Manogaran PS, Al-Hussein K, Platanius LC, Gutierrez MI, Bhatia KG. 2005. Curcumin suppresses growth and induces apoptosis in primary effusion lymphoma. *Oncogene* **24**:7022–7030.
31. Gururajan M, Chui R, Karuppanan AK, Ke J, Jennings CD, Bondada S. 2005. c-Jun N-terminal kinase (JNK) is required for survival and proliferation of B-lymphoma cells. *Blood* **106**:1382–1391.
32. Cohen A, Brodie C, Sarid R. 2006. An essential role of ERK signalling in TPA-induced reactivation of Kaposi's sarcoma-associated herpesvirus. *J. Gen. Virol.* **87**:795–802.
33. Ford PW, Bryan BA, Dyson OF, Weidner DA, Chintalgattu V, Akula SM. 2006. Raf/MEK/ERK signalling triggers reactivation of Kaposi's sarcoma-associated herpesvirus latency. *J. Gen. Virol.* **87**:1139–1144.
34. Qin Z, DeFee M, Isaacs JS, Parsons C. 2010. Extracellular Hsp90 serves as a co-factor for MAPK activation and latent viral gene expression during de novo infection by KSHV. *Virology* **403**:92–102.
35. Xie J, Ajibade AO, Ye F, Kuhne K, Gao SJ. 2008. Reactivation of Kaposi's sarcoma-associated herpesvirus from latency requires MEK/ERK, JNK and p38 multiple mitogen-activated protein kinase pathways. *Virology* **371**:139–154.
36. Pan H, Xie J, Ye F, Gao SJ. 2006. Modulation of Kaposi's sarcoma-associated herpesvirus infection and replication by MEK/ERK, JNK, and p38 multiple mitogen-activated protein kinase pathways during primary infection. *J. Virol.* **80**:5371–5382.
37. Sharma-Walia N, Krishnan HH, Naranatt PP, Zeng L, Smith MS, Chandran B. 2005. ERK1/2 and MEK1/2 induced by Kaposi's sarcoma-associated herpesvirus (human herpesvirus 8) early during infection of target cells are essential for expression of viral genes and for establishment of infection. *J. Virol.* **79**:10308–10329.
38. Haura EB, Turkson J, Jove R. 2005. Mechanisms of disease: insights into the emerging role of signal transducers and activators of transcription in cancer. *Nat. Clin. Pract. Oncol.* **2**:315–324.
39. Hirano T, Ishihara K, Hibi M. 2000. Roles of STAT3 in mediating the cell growth, differentiation and survival signals relayed through the IL-6 family of cytokine receptors. *Oncogene* **19**:2548–2556.
40. Punjabi AS, Carroll PA, Chen L, Lagunoff M. 2007. Persistent activation of STAT3 by latent Kaposi's sarcoma-associated herpesvirus infection of endothelial cells. *J. Virol.* **81**:2449–2458.
41. Morris VA, Punjabi AS, Lagunoff M. 2008. Activation of Akt through gp130 receptor signaling is required for Kaposi's sarcoma-associated herpesvirus-induced lymphatic reprogramming of endothelial cells. *J. Virol.* **82**:8771–8779.